Construction process induced vibrations on underground structures

I.Thusyanthan & S.P.G. Madabhushi
Department of Engineering, University of Cambridge,UK

ABSTRACT: Vibrations produced on the ground surface by engineering construction processes can damage underground structures. At present there is little knowledge of the level of surface vibrations that could cause damage to underground structures. The relevant British Standards, BS 5228 and BS 7385, have little reference to underground structures. Investigation of the soil-underground structure interaction, under ground borne vibration, must be carried out in a geotechnical centrifuge where prototype stresses and strains are recreated in the model. In this paper we discuss preliminary findings based on 1g experiments on small-scale models. Even though these tests were carried out at low stresses, useful information on the interaction aspects of underground structures was obtained. Experiments were carried out at 1g in a sand model instrumented with an array of miniature accelerometers around two model tunnel inclusions with brass and plastic tunnel linings. Impulsive and harmonic loadings were produced on the sand model surface by a drop hammer mechanism and an electric eccentric-mass motor respectively. The propagation of waves in dry sand and the vibration levels in model tunnels under both the impulse and harmonic surface loading were investigated.

1 INTRODUCTION

Engineering construction processes such as piling, blasting, dynamic compaction and demolition produce vibrations to varying degrees. These vibrations are transmitted through the ground as different types of stress wave. When these waves encounter an obstacle such as an underground structure, part of the wave energy is reflected and the rest is transmitted into the structure. The energy transmitted into the structure increases the stress level in the lining of the underground structure. This increase in stress level is usually small compared to the static stresses already present in the structure but since these induced stresses are cyclic in nature they can lead to fatigue cracks and cause damage to underground structures in the long term. Thus it is important to fully understand the propagation of waves through the soil and the transmission of soil vibrations into underground structures.

There are numerous research papers in the literature on the generation and propagation of waves in a half-space; many empirical equations are available to predict the magnitude of vibration away from the source. But there is very little work on the prediction of vibration amplitude in the presence of an underground structure. The relevant empirical equations can be used more effectively with a better understanding of how the presence of an underground structure alters the frequency and amplitude characteristics of the waves. A structure is damaged when the dynamic strains superimposed on the existing strains exceed the tolerance of the structure. The dynamic strain is proportional to the peak particle velocity (ppv). Hence ppv is used to specify the limit on ground vibration that can cause damage to a structure.

Even though the British standards BS 5228 (Part 4:- Code of practice for noise and vibration control applicable to piling operations), BS 7385 (Part 2 :- Evaluation and measurement for vibrations in buildings) and the draft Euro code EC3 provide guidance on vibration levels to prevent building damage, there are insufficient case histories to substantiate the guide values. Standards have little or no reference with regard to underground structures. This is mainly due to two reasons. Firstly, underground structures are considered to have a lower degree of risk of damage than the structures above the ground. Secondly, there had not been any recorded major damage to an underground structure due to construction process induced vibrations. This may be because of the present over-conservative limits. However with increased demand on land in major cities, piling operations may need to be undertaken very close to existing underground structures. This demands a thorough understanding of construction process induced vibrations on underground structures.

2 APPARATUS AND EXPERIMENTAL TECHNIQUES

2.1 *Overview*

Wave propagation in dry sand was studied using impulse and vibrating surface loads on dry sand placed in a 850mm tub. The impulse load was generated by means of a drop hammer mechanism while the vibrating load was generated by an electric eccentric-mass motor.

The 850mm diameter tub was used in all the experiments. Accelerometers, buried at several locations, were used to measure the vibrations in sand. DaisyLab software was used to log the acceleration signals from the accelerometers onto a computer. Experimental apparatus is shown in Figure 1.

Understanding how much of the soil vibration is transferred into an underground structure and how the presence of the structure alters the vibration levels in its vicinity are of real importance. Study in this area was carried out using two model tunnels, made of brass and plastic, placed in the sand tub. All the experiments were carried out at 1g.

2.2 *Vibration sources*

Two types of vibration sources were used in the experiment:- impulse load and vibrating load.

2.2.1 *Impulse load*

The impulse load was generated by dropping a 5kg mass from a height of 40mm. The drop hammer is controlled by means of a pneumatic switch. When the switch is off, low pressure is created in the vent connected to the hammer; hence the hammer is held in a retracted position. When the switch is on, atmospheric pressure is let into the vent and the hammer falls under gravity onto the base plate (aluminium plate 150mm x 90mm x 15mm), which is placed on the surface of sand.

2.2.2 *Vibrating load*

An electric motor with an eccentric rotating mass was used to produce the vibrations on the sand surface. The frequency of the electric motor was 50Hz. The motor was attached to the same base plate, which was used in the impulse load. Two accelerometers were attached to the base plate to record both the horizontal and vertical acceleration-time histories. The base plate experiences a peak particle acceleration of 3g in both horizontal and vertical directions (Fig. 4). This corresponds to component peak particle velocity of 93.7mm/s.

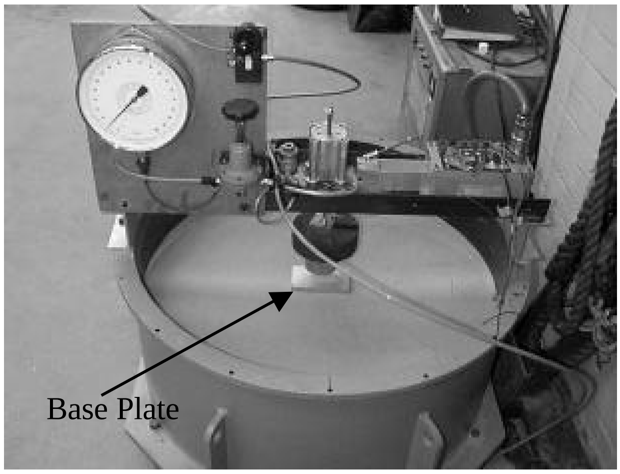

Figure 1. Impulse hammer mechanism on top of sand tub.

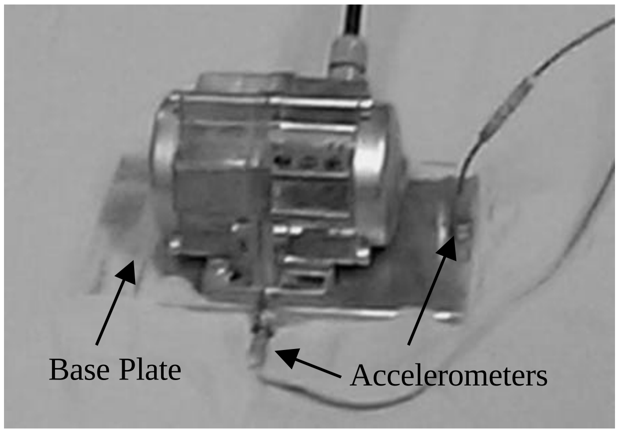

Figure 2. Vibrating motor attached to base plate.

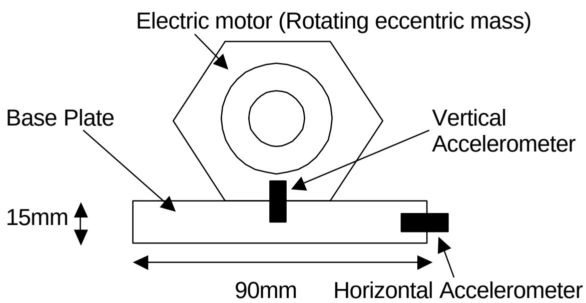

Figure 3. Cross section of vibratory motor and base plate

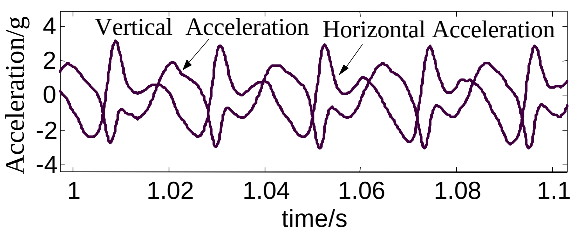

Figure 4. Base plate acceleration versus time.

2.3 *Model preparation and soil type*

The quality of the results obtained in the experiment depends directly on the quality of the model. Each time the model was made, the sand was poured into the model with the aid of a hopper. This was to make sure that the sand had the same void ratio and uniformly distributed packing in all the tests. A void ratio of 0.75 was aimed at all the models. LB 100/170 grade E dry sand was used in the experiments. It is uniformly graded sand.

2.4 *Data acquisition and filtering*

Signals from the accelerometers were acquired and recorded using DaisyLab software. A sampling rate of 10kHz per channel was used. The recorded data was post processed using MATLAB before it was used for analysis. Post processing involved eliminating zero-error in the signals and filtering. A butterworth filter was used to eliminate high frequency components above 500Hz.

2.5 *Model tunnels*

Two model tunnels with the same geometry, but different materials, were used in the experiment. The model tunnels, with diameter 54mm and length 320mm, were made of brass and plastic. Brass and plastic were chosen because they have contrasting impedance mismatches with sand (Table 1). Each model had two standard M6 holes at right angles. Accelerometers were securely fastened into these holes to measure the vibrations transmitted into the tunnel from the soil.

Table 1. Impedance of four media.

Media	Density kg/m^3	V_p * m/s	Impedance kg/m^2/s x 10^3
Sand	1525	159	242
Plastic	950	996	946
Brass	7500	4440	33300
Concrete	2400	3316	6163

* Pressure wave velocity

2.6 *Experimental setup*

12 accelerometers were used in the experiments. 6 accelerometers were placed horizontally at required locations to measure the horizontal accelerations; 6 other accelerometers were placed vertically at exact mirror locations. Three sets of experiments were carried out: Set A, to measure both horizontal and vertical acceleration in dry sand, and Sets B and C to measure the horizontal and vertical acceleration signals in the tunnels and at the tunnel vicinity. 10 tests were carried out in each set (5 impulse load tests and 5 vibratory load tests). Cross sectional views of the models used in experiment sets A, B and C are shown in figure 5. Each test is named using two letters and a test number. First letter represents the set; the second letter represents the type of load (i.e. AV3 - Set A, Vibrating load & Test 3).

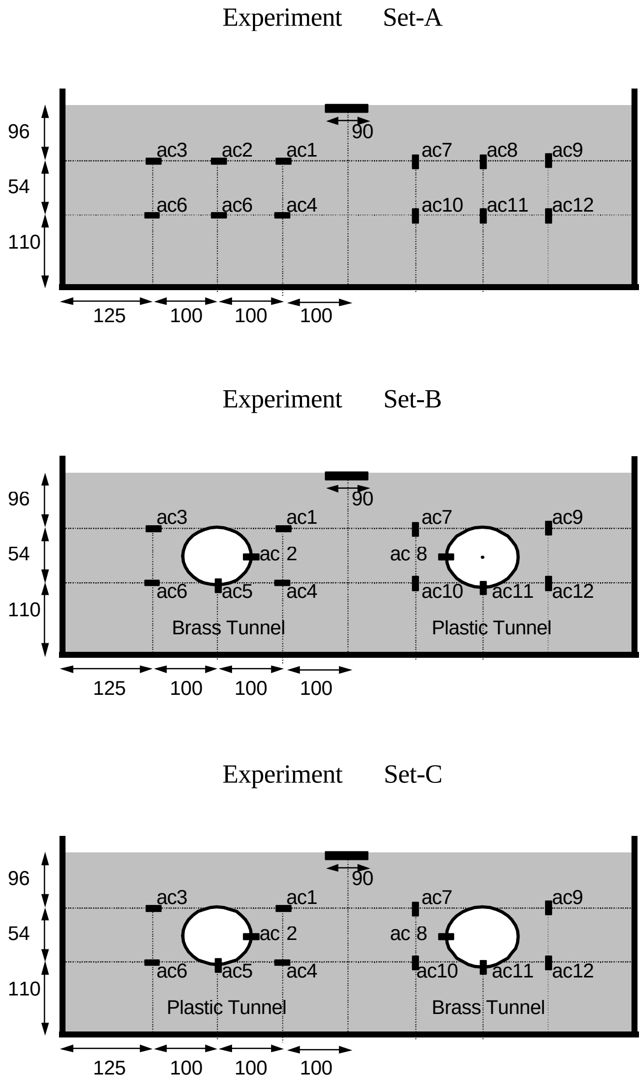

Figure 5. Cross sections of models

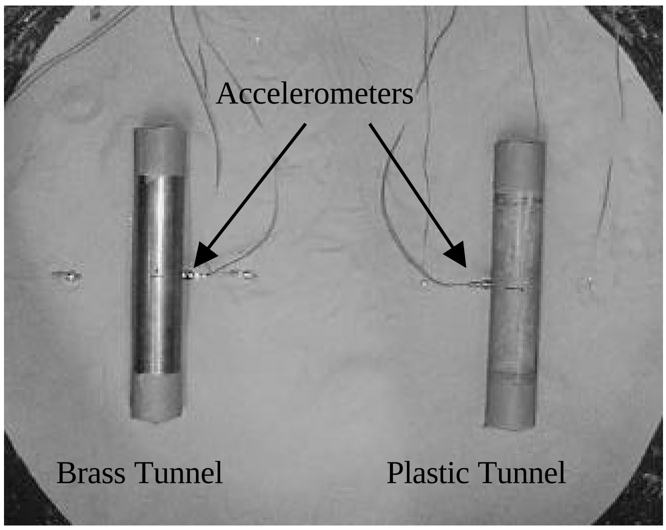

Figure 6. Plan view, preparation of model for set B experiment

3 RESULTS AND DISCUSIONS

3.1 *Results from set A experiment*

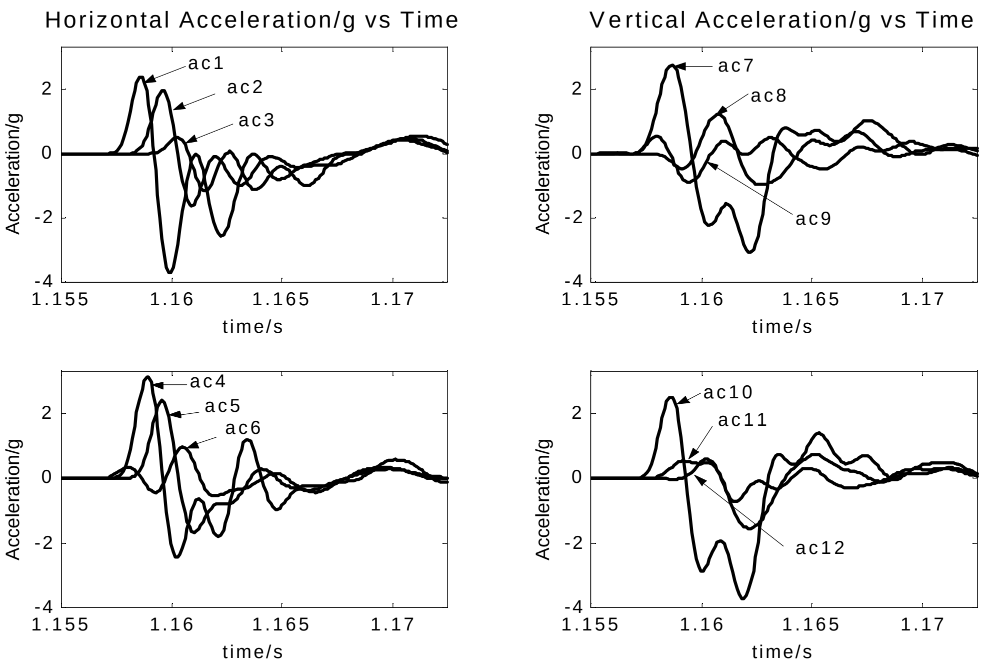

Figure 7. Acceleration signals under impulse load.

3.1.1 *Wave fronts from Impulse source*

Resultant peak particle accelerations (ppa) were obtained using horizontal and vertical peak particle accelerations. The resultant ppa was then normalized by the input vertical ppa of the base plate for each experiment in Set A. The average of the normalized ppa at each location, from the five experiments in Set A is plotted below in figure 8. Since sand particles were at rest before the impulse was applied, the direction of peak particle velocity (ppv) would be same as the direction of the ppa. Hence the wave fronts would be at right angles to the ppa vectors. The results agree well with the conventional theory which states that the compression waves propagate radially outwards from the source along a hemispherical wave front (Woods, 1969).

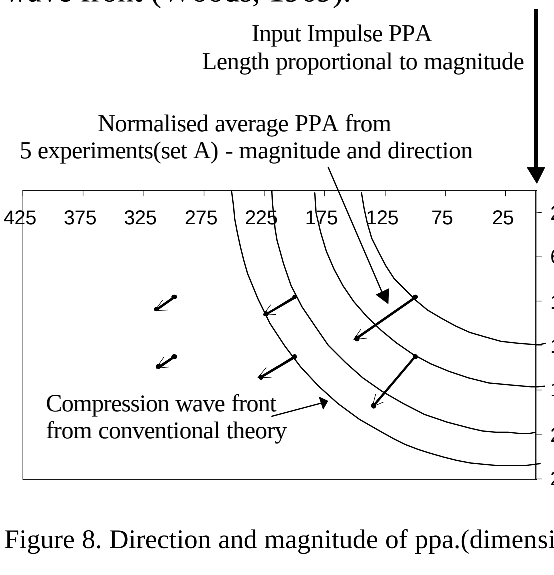

Figure 8. Direction and magnitude of ppa.(dimensions in mm)

3.1.2 *Peak particle velocity (ppv)*

Acceleration signals from vibratory load tests were integrated to obtain the velocity-time graphs for all the accelerometer signals. The zero-error in the acceleration signals varies with time. Hence the velocity signal, which results from integrating the acceleration signal, has a non-zero and time-varying mean. This makes the determination of the ppv slightly difficult, but the ppv can be found as half the maximum fluctuation in the velocity signal. Ppv's were obtained from all the signals. Horizontal and vertical ppv's were used to calculate the resultant ppv at the six locations. Resultant ppv's were then normalized using the input vertical ppv of the base plate for each experiment. If we consider spherical wave fronts advancing from the source, then the rate of attenuation of wave energy intensity, due to geometric spreading, would be proportional to $1/s^2$ where s is the slope distance from the source. Peak particle velocity of a wave is proportional to the square root of the energy of the wave. Hence in the absence of material damping, assumable in the present case as the distances between the source and the accelerometers are small, ppv would be expected to diminish as 1/s. Drawing these lines on the graph shows that the experimental results agree well with the line: - normalized ppv = 9/S (Fig. 9). In this equation, the input energy of the source and the soil condition parameter are both represented by a single value 9.

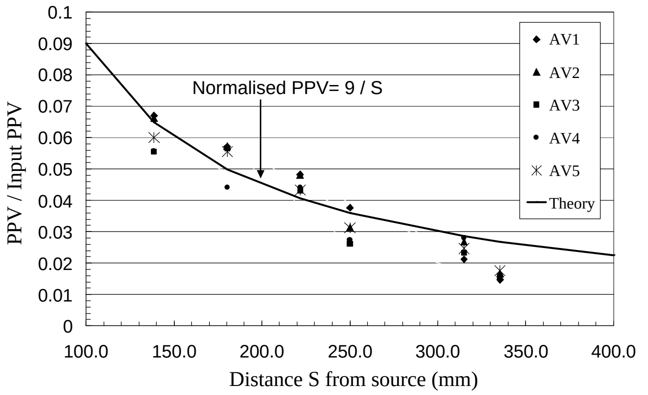

Figure 9. Normalised ppv versus slope distance S from source- results from set A experiments under vibratory load.

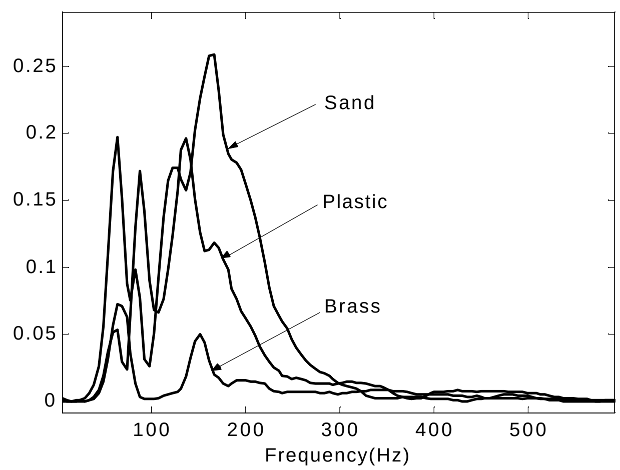

Figure 11. Power spectrum of vertical acceleration signal (ac11) under impulse load.

3.2 *Vibration level in model tunnels (results from set B & C experiments)*

It is clear from figure 10 below that the plastic model tunnel experiences higher peak acceleration in both the horizontal and vertical directions than the brass model tunnel. Specifying the peak acceleration is one way to quantify the difference in the acceleration signals in brass and plastic tunnels, but this does not represent the entire signal. Hence, a better way to quantify the difference in the signals would be to compare the area under the power spectrum of the acceleration signals. The area under the power spectrum represents the energy in the acceleration signal. Thus the ratio of the areas of the power spectrums would represent the energy ratios of the acceleration signals in brass and plastic tunnel.

3.3 *Power spectrum analysis*

Figure 11 shows a typical power spectrum of the vertical acceleration signal (ac11) in sand, plastic and brass under impulse surface loading. All three power spectral graphs show two distinct peaks at around 75 Hz and 150 Hz. This corresponds to the natural frequency of the soil in the model, which was calculated to be 75 Hz, and its first harmonic 150 Hz. This shows that the natural frequency of the soil plays a major part in the frequency content of the acceleration experienced by an underground structure.

The average value for the ratio of the power spectral area Brass/Plastic, from ten impulse tests (Table 2), was calculated to be 0.72. Similar power spectral analyses were performed on the acceleration signals from the vibratory load tests.

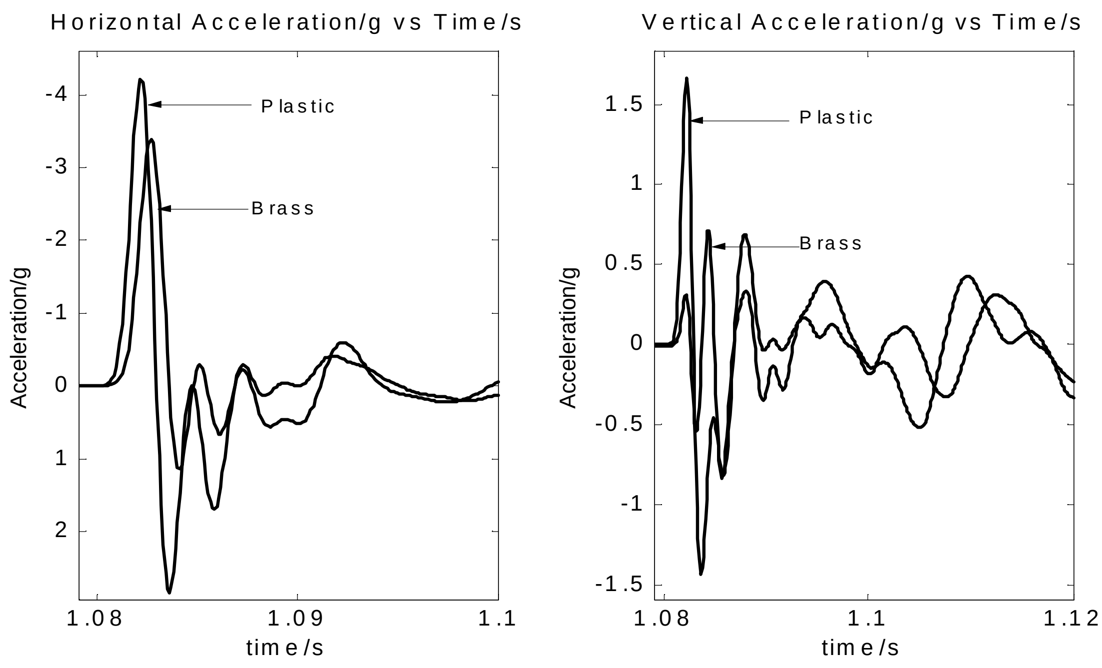

Figure 10. Acceleration signal from Plastic and Brass model tunnels (test CI2)

Table 2. Ratio of power spectral area for vertical acceleration signal under impulse surface load.

Test	Ratio of power spectral area Brass/Plastic	Test	Ratio of power spectral area Brass/Plastic
BI1	0.60	CI1	0.29*
BI2	0.73	CI2	1.00*
BI3	0.72	CI3	0.71
BI4	0.69	CI4	0.81
BI5	0.64	CI5	0.86

* These results were excluded in the average, as they do not follow the general trend.

The average value for the ratio of the power spectral area Brass/Plastic, from ten vibratory tests (Table 3), was calculated to be 0.73. Figure 12 shows a typical power spectrum of the vertical acceleration signal in plastic and brass under vibratory surface loading. The power spectrum of the signal in sand is not shown, as it is very similar to that of plastic but with higher magnitude. It is evident from the power spectrum that the vertical acceleration signal of the brass tunnel has the most energy near 100Hz while that of the plastic tunnel has the most energy near 150Hz. This trend is also exhibited in figure 11. This suggests that brass and plastic transmit energy at different frequencies in addition to the fact that they transmit different quantities of energy.

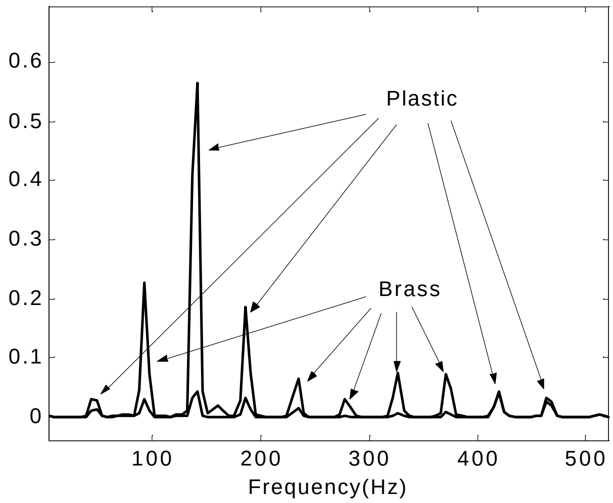

Figure 12. Power spectrum of vertical acceleration signal (ac11) under vibratory load.

Table 3. Ratio of power spectral area for vertical acceleration signal under vibratory surface load.

Test	Ratio of power spectral area Brass/Plastic	Test	Ratio of power spectral area Brass/Plastic
BV1	0.76	CV1	0.79
BV2	0.68	CV2	0.82
BV3	0.62	CV3	0.75
BV4	0.67	CV4	0.73
BV5	0.75	CV5	0.75

The impedance mismatch between the sand and the tunnel determines the amount of wave energy transmitted into the tunnel. The impedance mismatch between sand and brass is greater than that between sand and plastic. Hence more energy will be transmitted into plastic tunnel. Results from the above power spectral analysis suggest that energy transmitted into a brass tunnel is 72.5% of that transmitted into a plastic tunnel.

An alternative method to quantify the ratio of energy transferred into the model tunnels is to use peak particle velocity. Acceleration signals were integrated to obtain the velocity-time graphs. Peak particle velocities were obtained from all the velocity–time graphs. Table 4 summarises the ratio of ppv in brass to plastic in all ten tests. The average ratio of ppv in brass to plastic was calculated to be 0.82.

Table 4. . Peak particle velocity (mm/s) of model tunnels in vertical direction.

Test	Brass ppv mm/s	Plastic ppv mm/s	Brass ppv / Plastic ppv
BV1	1.40	1.80	0.78
BV2	1.50	1.75	0.86
BV3	1.30	1.50	0.87
BV4	1.35	1.60	0.84
BV5	1.25	1.40	0.89
CV1	1.25	1.50	0.83
CV2	1.22	1.50	0.83
CV3	1.18	1.30	0.90
CV4	1.10	1.40	0.79
CV5	0.90	1.40	0.64

3.4 *Relationship between energy transferred and impedance mismatch*

Energy transferred into the model tunnel is proportional to the square of the peak particle velocity in the model tunnel. Hence the ratio of energy transferred into the model tunnels can be calculated using the ppv ratio of brass to plastic.

$$\frac{\text{Energy transferred into Brass model tunnel}}{\text{Energy transferred into Plastic model tunnel}}$$

$= 0.82^2 \quad = 67\ \%$

We can try to correlate the impedance mismatch ratio to the square of the ppv ratio. Table 1 shows the impedances of four media. Let the impedance of sand, plastic and brass be I_s, I_p and I_b respectively. The following relationship is proposed:

$$\left[\frac{Brass's\ \ ppv}{T's\ \ ppv}\right]^2 = \left[\frac{I_T - I_s}{I_b - I_s}\right]^n \qquad (1)$$

where n is a constant; T is a model tunnel whose impedance is between that of brass and plastic. Figure

13 shows the above relationship lines for n=0.05, 0.1 and 0.15. Note that all three lines pass through the boundary condition (i.e. the ratio of energy transferred is one when the ratio of impedance mismatch is one). It can be seen from figure 13 that the line corresponding to n=0.1 agrees well with the experimental point for plastic (ratio of brass to plastic ppv squared = 0.67).

Figure 13 can be used to predict energy transferred into a material T at shallow depths (at low soil stresses). Thus we can predict that the ratio of energy transferred into a brass tunnel to a concrete tunnel, at shallow depths, is 0.86.

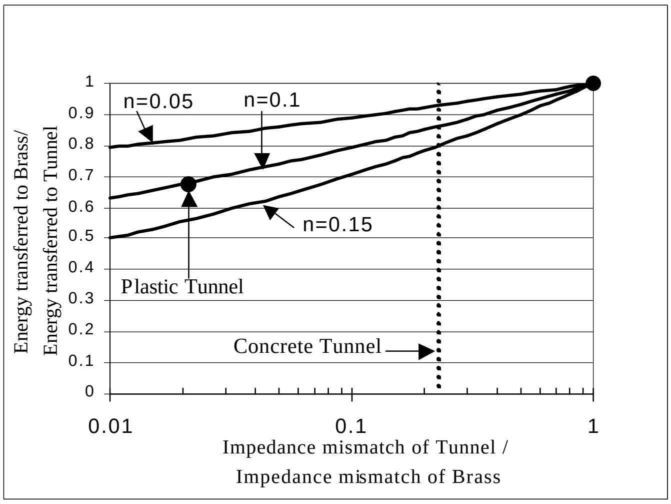

Figure 13. Ratio of Energy transferred vs ratio of impedance mismatch

4 CONCLUSION

The tunnel lining has an important role to play in determining the amount of energy absorbed from ground borne vibrations. The vibration amplitude transferred into the plastic tunnel was shown to be higher than that transferred into the brass tunnel under impulse and harmonic loads. Under harmonic loading, the plastic model tunnel appeared to absorb energy at higher frequencies (150Hz-200Hz) relative to brass model tunnel (100Hz). Experimental results show that the ratio of peak particle velocity (vertical) in the brass tunnel to the plastic tunnel is 0.82. Hence the ratio of energy transferred into the brass tunnel to the plastic tunnel, which is the square of ppv ratio, is 0.67.

It is also worth remembering that the damage to an underground structure is not only dependent on the amount of energy transferred into the structure but also on the frequencies at which the energy is transferred.

The following relationship is proposed for the impedance mismatch ratio and the square of the ppv ratio (i.e ratio of the energy transferred).

$$\left[\frac{Brass's\ \ ppv}{T's\ \ ppv}\right]^2 = \left[\frac{I_T - I_s}{I_b - I_s}\right]^{0.1} \qquad (2)$$

The above conclusions can form the basis on which more research can be carried out to expand the knowledge in this field. The energy transfer into various tunnel linings such as pre-cast concrete, shotcrete and steel can also be investigated. Thorough study in this field will enable us to understand and improve on the vibration limits set out by the present British Standards.

REFERENCES

Chao, C.-C.(1960) *Dynamical response of an elastic half-space to tangential surface loadings*. J. appl. Mech. 27, 559-67.

Head J.M and Jardine F.M.(1992) *Ground borne vibrations arising from piling*. CIRIA-Technical Note 142.

Hiller D.M. and Bowers K.H.(1997). *Groundborne vibrations from mechanized tunnelling works*. Proceedings of Tunnelling 97, Institution of Mining and Metallurgy, London, 1997, 721-735.

Hope V.S and Hiller D.M.(1998) *The Prediction of ground-borne vibration from percussive piling*. Canadian Geotechnical Journal, Vol-37,Pg 700-711.

Hudson. J.A (1980) *The excitation and propagation of elastic waves*. Cambridge University Press.

Karl F.Graff (1975). *Wave motion in Elastic solids* . Oxford University Press.Pg 395-410.

Madabhushi S.P.G and Steedman R.S.(1989). *Wave transmission at a multi-media interface*. Technical report, CUED/D-SOILS/TR227, Cambridge University.

Miller, G.F. and Pursey, H.(1954) The Field and the radiation impedance of mechanical radiators on the free surface of a semi-infinite isotropic solid. Proc.R.Soc A223, 521-41.

Thusyanthan, I. (2001) *Construction process induced vibrations on underground structures*. MEng Project Report, Cambridge University.

Woods R.D, Richard F.E, Hall J.R.(1969).*Vibrations of soils and foundation*. Prentice-Hall.